A REALTIME CLOSE-RANGE IMAGING SYSTEM WITH FIXED ANTENNAS

B. Michael, W. Menzel

Microwave Techniques, University of Ulm, PO Box, D-89069 Ulm, Germany

ABSTRACT

A coherent system with two stepped frequency radar sensors separated by 1 - 2 m is presented for close range imaging. Resolution is achieved via range resolution from the two different sensor positions, exploiting both mono- and bistatic responses. First test had been made using a vector measurement equipment for an antenna measurement range as radar simulator, and now, a mobile experimental system was built up and tested including stationary and mobile targets.

INTRODUCTION

Imaging of different scenes, even under adverse environmental conditions, is playing an important role for a number of applications like autonomous vehicles (robots) or as a collision warning for cars driving forwards or backwards or changing the lane [1] - [6]. In a number of these scenarios, an imaging of the relevant area around the vehicle has to be performed. In most cases, this is done by a scanning antenna with a narrow beamwidth in azimuth [4], [5]. This, however, requires antennas with relatively large lateral dimensions combined with mechanical [4] or electronic scanning, e. g. frequency scanning [5], resulting in large and expensive antenna arrangements. For close-range imaging, on the other hand, an imaging is possible, too, by doing separate measurement from at least two different positions via range, using wide beamwidth antennas. Therefore, a novel system for close-range imaging was proposed using two antennas separated by 1 to 2 m [7]. In the meantime, a mobile experimental radar system has been built and tested. The original imaging algorithms have been extended to detect and correctly determine both location and speed of moving targets.

IMAGING PRINCIPLE

The proposed arrangement consists of two radar sensors separated by approximately the width of the respective vehicle. The antennas have a wide beam in azimuth whereas a narrower beamwidth typically is desirable in elevation. To this end, H-plane waveguide horns including a lens for reduced length with horizontal polarization and beam widths of 77° in azimuth and 12° in elevation and a gain of about 15 dBi were employed. For a single target, each sensor gives a monostatic as well as a bistatic response according to the respective distance; taking into account reciprocity, three independent sets of data are available for each target described by two circles around each antenna and an ellipse with the antennas as focal points (Fig. 1). This already gives some means to separate multi-target scenarios; this can be improved considerably by employing a coherent sensor system. For system simplicity and for minimal EIRP, FMCW- or stepped frequency sensors are advantageous. For a stepped frequency system, a coherent evaluation of the measured data can be done by

$$A(P) = \left(\frac{1}{r_{1P}} \sum_{i=0}^{N-1} E_{i11} \cdot e^{j2k_i r_{1P}} \right) \bullet \left(\frac{1}{r_{2P}} \sum_{i=0}^{N-1} E_{i22} \cdot e^{j2k_i r_{2P}} \right) \bullet \left(\frac{1}{\sqrt{r_{1P} \cdot r_{2P}}} \sum_{i=0}^{N-1} E_{i12} \cdot e^{jk_i (r_{1P} + r_{2P})} \right) \quad (1)$$

where A(P) is the amplitude at a possible target at point P, E_{i11} and E_{i22} are the received electric fields at frequency step i at antenna 1 and 2, respectively, transmitted by the same antenna. The third term of this equation represents the bistatic response; E_{i12} could equally be replaced by E_{i21} due to reciprocity.

r_{1P} and r_{2P} are the distances between antenna 1 or antenna 2 and the target. For a range dependent amplitude correction, the far field approximation of the Hankel function for cylindrical problems is assumed. The summation is done over the number N of measured frequency points. The overall measurement bandwidth Δf determines the sensor resolution $\Delta R = c_0 / (2\Delta f)$, while N determines the unambiguous range of the sensor system $R_{unamb} = N \cdot \Delta R$. Possible frequencies of operation may be around 24 GHz, 61 GHz, or 77 GHz. For the test system described here, 24 GHz were chosen.

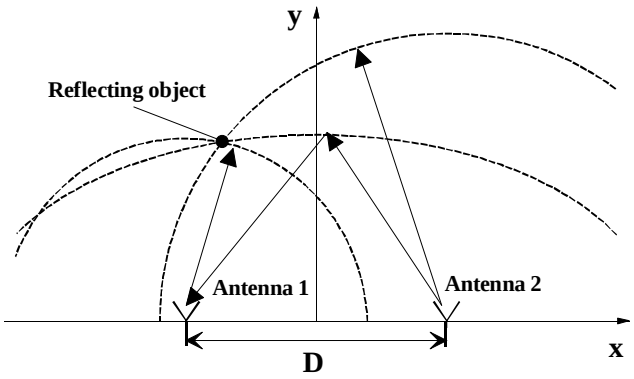

Fig. 1: Basic principle of the imaging sensor.

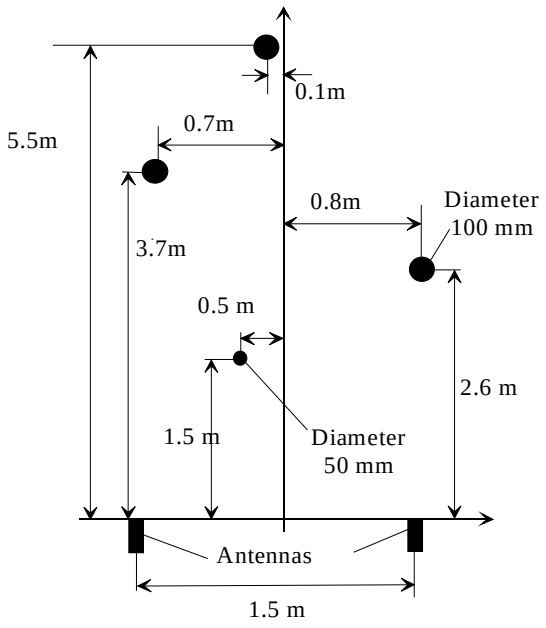

Fig. 2: Geometrical arrangement of 4 metal cylinders.

STATIONARY MEASUREMENTS

Using an antenna range with a vector network analyzer as measurement system and an offline data processing, preliminary tests with varying bandwidths have been made. An arrangement consisting of four metal cylinders is shown in Fig. 2, and the related radar image is plotted in Fig. 3 for a 11 GHz as well as a 1 GHz bandwidth. The arrangement of the targets can be clearly recognized. For increasing distance, the system response is widened which can easily be explained by the geometrical representation in Fig. 1; the angles between the two circles and the ellipse become increasingly smaller. With this equipment, however, acquisition time is rather long, and only measurements of static targets close to the laboratory could be done.

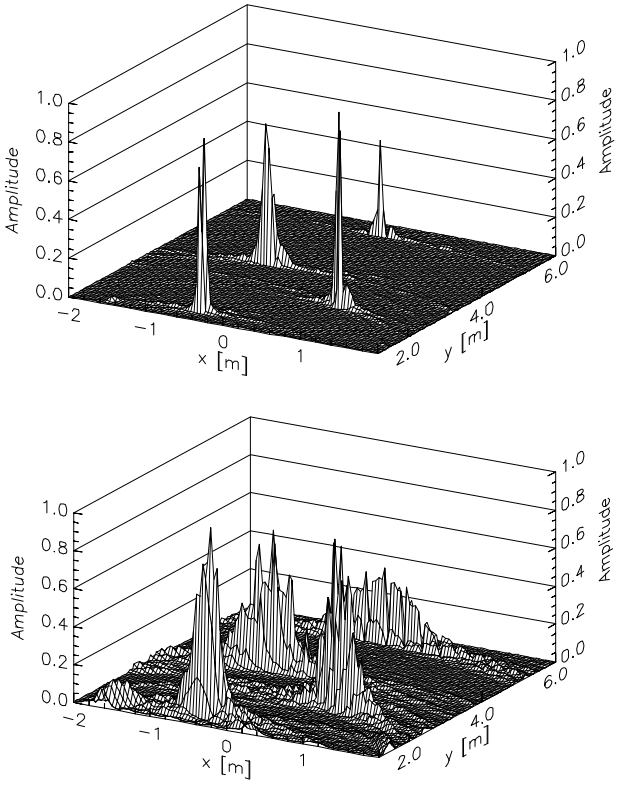

Fig. 3: Images of 4 cylinder arrangement according to Fig. 2 with bandwidths of 11 GHz (top) and 1 GHz (bottom).

MOBILE REAL-TIME SENSOR SYSTEM

To evaluate the imaging principle presented above in arbitrary scenarios and including realistic, e.g. moving targets, an experimental system was built and tested. A block diagram of the radar sensor is given in Fig. 4. Separate antennas were used for transmit and receive to improve TR isolation, and a bandwidth of 500 MHz was chosen as a compromise between resolution, possible PTT restrictions, and effort.

A first result for a situation similar to the tests in Figs. 2 and 3 is displayed in Fig. 5. Four posts situated on a small road can be recognized easily in the radar image.

To include moving targets, two steps were taken. The own speed of the vehicle with the radar sensor typically is known; a respective Doppler frequency correction easily can be included into the image processing. A more complex task is the detection of both speed (absolute value and direction) and location of an independently moving target within the imaging range.

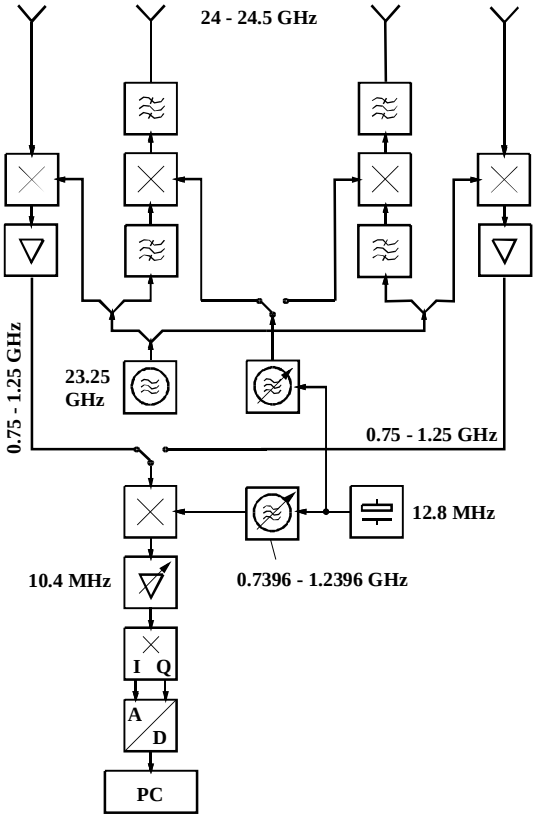

Fig. 4: Block diagram of the real-time mobile radar sensor.

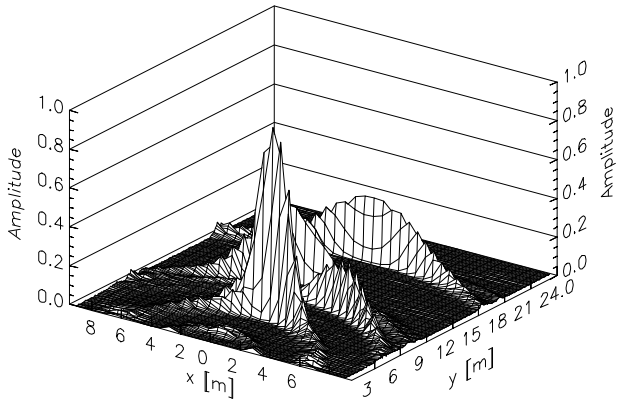

Fig. 5: Photograph and radar image of a four post scene.

Without any measure, a rather disturbed image of a moving car results, as shown in Fig. 6 (top). To solve this problem, the signal processing algorithm is modified. In a first step, a number of measurements are done at a single frequency, from which the radial Doppler frequencies are determined with respect to the monostatic and the bistatic responses. (As a further improvement, the extraction of the Doppler information from the frequency stepped mode will be investigated). Then the normal stepped frequency measurements are done. The evaluation of these measurements, however, is performed using a phase correction to account for the Doppler frequency and the phase change due to the movement of the target between the single measurement steps. As the position of the target still is unknown, and only the radial speed components are known (they add up to different speed vectors for different target locations), a potential speed vector is determined for each cell of the image area, and the imaging algorithm according

to equ. (1) is performed including a correction with respect to the assumed speed vector:

$$A(P) = \left(\frac{1}{r_{1P}} \sum_{i=0}^{N-1} E_{i11} \cdot e^{j2k_i r_{1P}} \cdot \underline{e^{j2\pi f_{D1} \cdot i \cdot \Delta t}} \right) \bullet \left(\frac{1}{r_{2P}} \sum_{i=0}^{N-1} E_{i22} \cdot e^{j2k_i r_{2P}} \cdot \underline{e^{j2\pi f_{D2} \cdot i \cdot \Delta t}} \right) \bullet \left(\frac{1}{\sqrt{r_{1P} \cdot r_{2P}}} \sum_{i=0}^{N-1} E_{i12} \cdot e^{jk_i (r_{1P} + r_{2P})} \cdot \underline{e^{j2\pi f_{DB} \cdot i \cdot \Delta t}} \right) \quad (2)$$

The correction factors are underlined. f_{D1}, $f_{D2,}$ and f_{DB} are the radial Doppler frequencies with respect to sensor 1 and 2 and the bistatic response, respectively, Δt is the time between two frequency steps. This correction is valid only if the target really is present in that cell; consequently, only at the real position of the target, amplitude is raised.

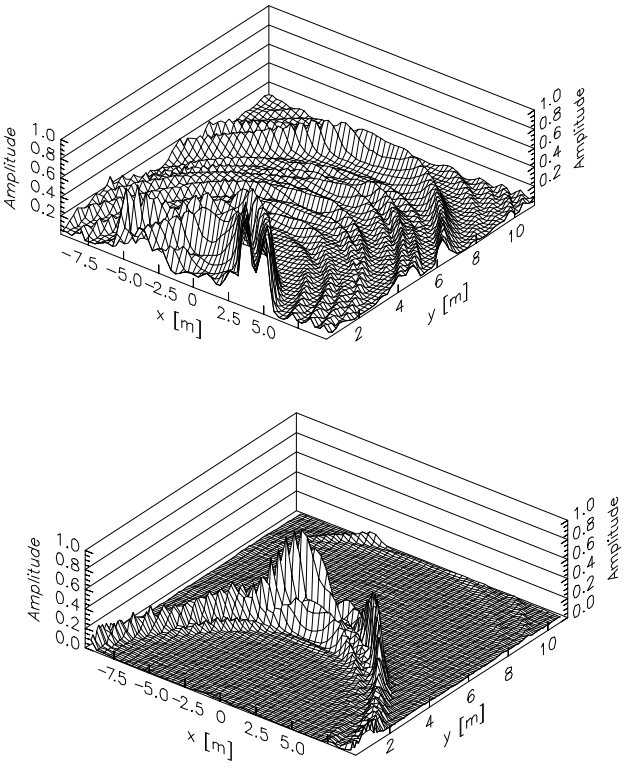

Fig. 6: Radar image of a moving car.
(Top: uncorrected data; bottom: Doppler corrected data according to equ. 2 {speed 5.5 km/h, distance 5.5 m}).

This now was done for the the moving car mentionned above. Now the two corners of the car clearly can be recognized (Fig. 6, bottom). The speed of this car was 5.5 km/s at a distance of 5.5 m.

CONCLUSIONS

The principle of a novel close range radar sensor for possible applications with small autonomous vehicles or as a automotive sensor for driving backwards has been demonstrated. A mobile test system has been built, and first results have been shown, including both stationary and a moving target.

REFERENCES

[1] H. H. Meinel: Applications of Microwaves and Millimeterwaves for Vehicle Communications and Control in Europe. IEEE Int. Microw. Symp. (MTT-S) 1992, Albuquerque, pp. 609 - 612.

[2] H. Daembkes, J. F. Luy: Millimetrewave components and systems for automotive applications. Microwave Engineering Europe (Dec.-Jan. 96), pp. 43 - 48.

[3] M. Kotaki et al.: Development of millimeter wave automotive sensing technology in Japan. IEEE int. Microw. Symp. (MTT-S) 1992, Albuquerque, pp. 709 - 712.

[4] M. Lange et al.: 94 GHz imaging radar for autonomous vehicles. 18th Europ. Microw. Conf., Stockholm, Sweden, 1988, pp. 826 - 830.

[5] A. G. Stove: 80 GHz Radar for Cars. Military Microw. Conf., London, 1992, pp. 389 - 394.

[6] H. T. Steenstra, F. L. Muller, P. J. F. Swart: Multistatic FMCW radar for collision avoidance applications, optimization of the antenna configuration and improving the data processing. 28th European Microw. Conf. 1999, Munich, Germany, Vol. II, pp. 13 – 16.

[7] B. Michael, W. Menzel: A Novel Close-Range Imaging System. 26th European Microw. Conf., Prague, 1996, pp.130 - 134.